J Mater Sci (2008) 43:3417–3423
DOI 10.1007/s10853-008-2463-y

NANOSMAT 2007 - INTERNATIONAL CONFERENCE ON SURFACES, COATINGS AND NANOSTRUCTURED MATERIALS

Effect of hydrogen content on the ZnO thin films on the surface of polyethylene terephthalate substrate through electron cyclotron resonance-metal organic chemical vapor deposition

J. H. Park · D. Byun · B. J. Jeon · J. K. Lee

Received: 5 July 2007 / Accepted: 8 January 2008 / Published online: 6 March 2008

Abstract Zinc oxide thin films were deposited on polyethylene terephthalate (PET) substrate by the electron cyclotron resonance-metal organic chemical vapor deposition (ECR-MOCVD) method at room temperature with the addition of hydrogen to the reaction gas. Diethyl zinc (DEZn) as the source precursor, O_2 as oxidizer and argon as carrier gas were used for the preparation of ZnO film. Scanning electron micrography and X-ray diffraction analyses revealed that the ZnO grains with size of ca. 20 nm had an elliptic cylindrical configuration and were highly *c*-axis-oriented. The hydrogen content strongly affected the crystallographic structure, electrical property, and composition, as well as the surface roughness of the zinc oxide films. The chemical composition and surface states of the films were further examined by RBS and XPS to find the reason for the different electrical resistivity with variation of H_2/Ar ratio. It can be concluded that hydrogen content plays an important role in increasing the Hall mobility, hole concentration, and electron concentration in our experimental range.

J. H. Park · J. K. Lee (✉)
Advanced Energy Materials Processing Laboratory, Battery Research Center, Korea Institute of Science and Technology, P.O. Box 131, Cheongryang, Seoul 130-650, Republic of Korea
e-mail: leejk@kist.re.kr

J. H. Park · D. Byun
Department of Materials Science & Engineering, Korea University, Seoul 136-701, Republic of Korea

B. J. Jeon
Epon Co., Ltd., 672, Sungkong-dong, Danwon-gu, Ansan city, Gyunggi-do 425-836, Republic of Korea

Introduction

The room temperature deposition of ZnO films on polyethylene terephthalate (PET) substrate enabled by the employment of ECR-MOCVD has attracted much attention for potential applications in flexible displays, curved circuits, optoelectronic devices, curved detector arrays, and in sensor skins. In any application, the plastic substrate provide devices that are lighter in weight and more resistant to impact damage, making them suitable for portable devices [1–4]. Zinc oxide has optical transmittance over 90% in the visible wavelength region as a transparent conductive oxide. It also could be used by an optical field due to the band gap in the range of 3.2–3.3 eV [5–12]. ZnO in the form of thin films on PET has many advantages, such as its lighter weight, smaller volume, lower cost, and flexibility when compared with deposition on glasses. For the deposition of ZnO on polymer, low temperatures are required for preparation due to thermal weakness of plastic materials. Besides, the adhesion between metallic layer and plastic substrate is critical to a variety of vacuum technologies [13–15]. In recent years, we have developed the ECR-MOCVD method by using an organometallic precursor at room temperature, in which a periodic negative voltage is applied beneath the polymer substrate [16–18].

We have studied the chemical vapor deposition of ZnO films at room temperature using organometallic precursors of diethyl zinc under ECR plasma. In this work, the relationship between the characteristics of the zinc oxide film and process parameters is investigated and their electrical properties are determined as a function of H_2/Ar mole ratio.

Experiment

The substrates used for the experiments were PET with a thickness of 0.1 mm samples were cut into 15 × 15 cm^2 squares. The nozzle stood at a distance of 2 cm from the substrate to spray the deposition zone with the reaction gas. The precursor, diethyl zinc (DEZn) with a purity of 99.9%, was used as the organometallic source. An ECR plasma system with two electromagnetic was employed to carry out the experiments. It consisted of two separate zones, the plasma zone and the deposition zone. The system was pumped down to a base pressure of 1×10^{-6} Torr with a turbomolecular pump, backed by a rotary mechanical pump and a Roots blower pump. The precursor, DEZn, was then introduced into the deposition chamber using Ar as a carrier gas. The carrier gas, Ar, flowed through the bypass line of the DEZn bubbler until the reactor was stabilized; then it flowed into the reactor through the DEZn bubbler, which was maintained at −10 °C. At the same time, H_2 gas was introduced directly into the reaction chamber. The ECR microwave plasma was generated using a microwave generator (2.45 GHz) coupled with a magnetic field (875 Gauss). The samples were prepared under the following conditions: a working pressure of 10 mTorr, O_2/Ar and H_2/Ar content ratios of 1.4 and 0–0.6, respectively, deposition time of 15 min, and microwave power of 850 W. The morphology and grain size of the films were determined through micrographs obtained using field emission-scanning electron microscopy (FE-SEM). The X-ray diffraction (XRD) studies were carried out in a Rigaku Miniflex diffractometer (Cu Kα radiation 1.5406 Å), with a thin film attachment. The surface topography analysis was performed by atomic force microscopy (AFM). The sheet resistance of the films was measured by a four-point probe, with appropriate geometric corrections. Also, the carrier concentration and mobility of the films were investigated by using Hall measurement equipment (HEM-1000). Transmittance spectra were obtained from 300 to 900 nm using a UV–VIS spectrophotometer. Photoluminescence (PL) spectroscopy was selected for the optical characterization of the ZnO films. The PL measurements were conducted at room temperature by means of a fluorometer, with a laser having an excitation wavelength of 350 nm. The chemical composition of the ZnO films was examined by X-ray photoelectron spectroscopy (XPS) and RBS (National Electrostatic, MEV in beam accelerator) with maximum 2 MV.

Results and discussion

Typical growth mechanism of ZnO film by the ECR-MOCVD are as follows In the first step, the electrons and hydrogen ions with high energy are generated by ion impacts and decomposition of the plasma gas in the ECR plasma zone. After the inelastic collisions of the DEZn molecules with electrons and ions, the activated DEZn can be hydrogenated. Zinc ions, carbon fragments, and hydrogen ions are generated by decomposition of the precursor. Most of zinc ions formed in the bulk plasma are maintained at a positive charge. The ZnO films are obtained from reacting these positive-charged zinc ions with negative charged oxygen ions in the plasma.

In order to understand how the mole ratio of H_2 to argon (Ar) affects ZnO nanostructure, we compared the surface morphologies of ZnO film on PET surface synthesized at five different conditions. Figure 1 shows the SEM images of the ZnO film obtained by ECR-MOCVD. It can be seen that the film is composed of nano-grains, which appear to be elliptic cylinders with an open packed structure. The ZnO grains that grow under an argon atmosphere (at $H_2/Ar = 0$) are about 12 nm in diameter and 65 nm in length. The length of the cylinder in Fig. 1a is not uniform over all specimens. This variation is possibly caused by rapid growth from high concentrations of zinc ions in and around the film surface [19]. The hydrogen plasma, generating in the reaction zone under hydrogen rich conditions, can supply high-density zinc ions to the surface atoms of the elliptic cylinders to promote the formation of larger diameter ZnO grain. The cross-sectional SEM images also show that the measured film thickness was about 400 nm. Introducing H_2 into the reactor increases the size of a ZnO grain but not the film thickness. The length of a grain increased up to ca. 160 nm gradually with an increasing H_2/Ar ratio and then remained constant for a H_2/Ar ratio of 0.45–0.6. The film thickness was constant at 600 nm with regardless of the change in H_2/Ar ratio. The increase of the H_2/Ar mole ratio is associated with the degree of decomposition of the zinc precursor, DEZn. The rods grow in size because energy from the excited hydrogen is transferred to the precursor of Zn, DEZn. However, too much hydrogen in the reactor may lead to etching of the film by excess ion bombardment of the surface. The constant film thickness observed, therefore, was due to a balance between hydrogen ion etching and a surface reaction of the decomposed zinc.

XRD patterns of the ZnO thin films deposited on PET at different H_2/Ar mole ratios are shown in Fig. 2. It can be seen that ZnO deposited with mixed orientation for (002), (100), (101), and (110) planes. From these results, we see that all X-ray diffraction peaks can be identified as a polycrystalline wurtzite-type structure of ZnO consistent with the values in the standard index (JCPDS 36–1451). With an increasing H_2/Ar mole ratio, the ZnO film takes on a preferred orientation of (002), while other orientations like (100), (101), and (110), are also seen with comparatively lower intensities.

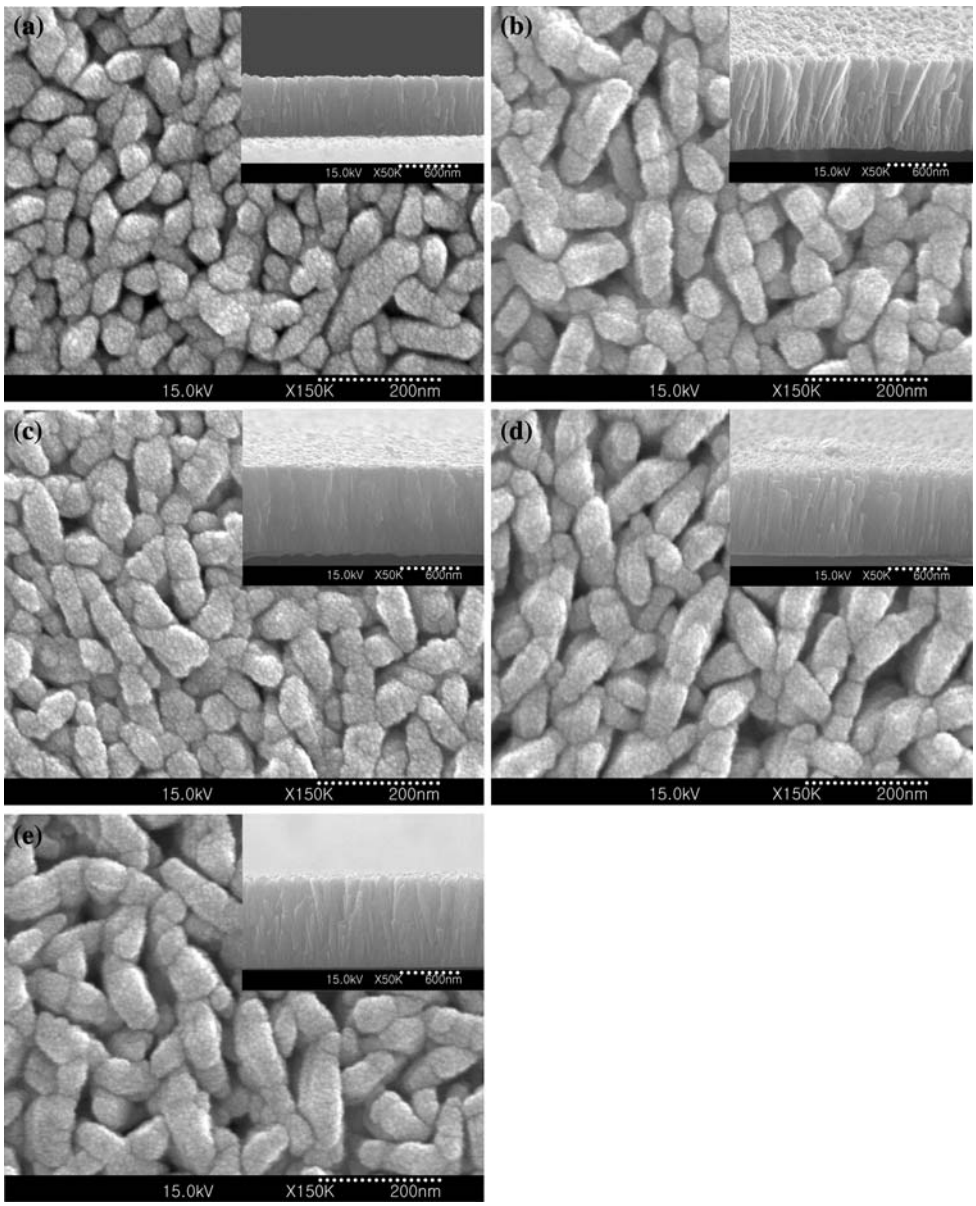

Fig. 1 SEM morphology of ZnO films deposited on PET by ECR-MOCVD with H_2/Ar ratio of (**a**) 0, (**b**) 0.15, (**c**) 0.3, (**d**) 0.45 and (**e**) 0.6. Microwave power of 850 W, magnetic current power of 160 A, distance from the magnet to the DEZn feeding point of 5 cm, distance from the DEZn feeding point to the substrate of 2 cm, working pressure of 10 mTorr, and a deposition time of 15 min

Therefore the crystallites are highly oriented with their *c*-axis perpendicular to the plane of the substrate. In addition, dominant signals associated with the (100) and (101) planes are found for ZnO films prepared in the presence of hydrogen. Crystallites size estimates for the ZnO thin films as a function of the H_2/Ar mole ratio were calculated from the (002) peaks in the XRD patterns. Measuring the full width at half-maximum (FWHM), crystallite sizes were estimated using the Debye–Scherer formula [20].

$$D = 0.9\lambda/B\cos\theta \quad (1)$$

where D is the crystallite size, λ is the wavelength value of the $CuK_{\alpha 1}$ line, θ is the Bragg diffraction angle and B is the FWHM of the diffraction peak measured in radians. As shown in the Table 1, only a slight decrease in the calculated crystallite size is observed with increasing H_2/Ar mole ratio. Therefore, the effect of H_2/Ar mole ratio on the crystallite size is insignificant.

Figure 3 shows the typical transmittance spectra for ZnO films on PET substrate in the visible range of 380–800 nm. When we compare the transmittance spectra for ZnO films of Fig. 3(a–e), a significant difference was not observed in the shorter wavelengths below 500 nm. The transmittance is about 90% in this range for all of the ZnO films. However, the transmittance of the ZnO film gradually decreased with an increase of wavelength and then increased slightly with a further increase of wavelength up to 700 nm. On the other hand, transmittance of ZnO films prepared without hydrogen (Fig. 3a) increased continuously up to maximum and then decreased slightly with an

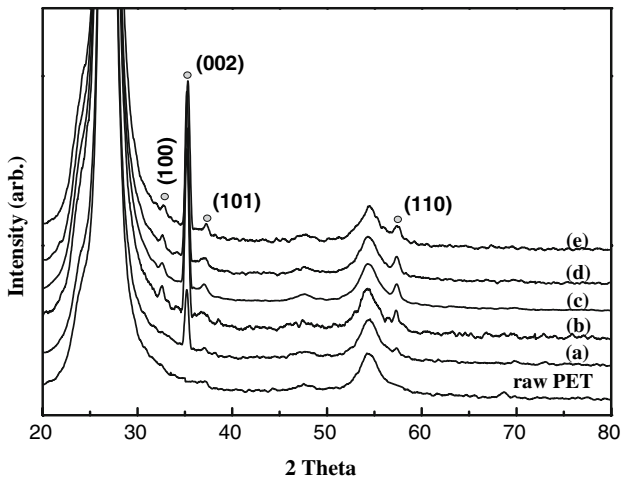

Fig. 2 X-ray diffraction patterns of ZnO thin films for various H_2/Ar ratio of (**a**) 0, (**b**) 0.15, (**c**) 0.3, (**d**) 0.45 and (**e**) 0.6

Table 1 Crystallite size and FWHM for ZnO film deposited at different H_2/Ar mole ratios

H_2/Ar mole ratio	FWHM	Crystallite size (nm) ± 10%
0	0.682	21.33
0.15	0.682	21.32
0.3	0.706	20.60
0.45	0.706	20.60
0.6	0.706	20.60

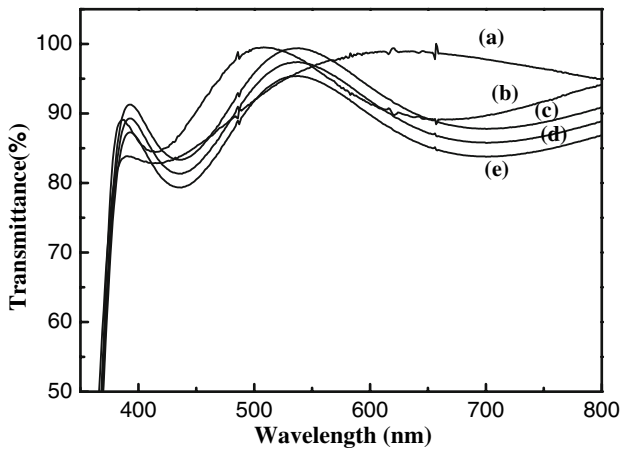

Fig. 3 Transmittances of ZnO film prepared by ECR-MOCVD with H_2/Ar ratios of (**a**) 0, (**b**) 0.15, (**c**) 0.3, (**d**) 0.45 and (**e**) 0.6

increase of wavelength. The lower transmittance of ZnO films in the presence of hydrogen is attributed to the large particle size, which causes light scattering through higher surface roughness. These results possibly may be explained by a quantum confinement effect that arises from differences in crystalline size [21].

Figure 4 shows the photoluminescence spectra of ZnO obtained at room temperature in the photon energy range from 2.5 to 3.5 eV using an excitation photon energy (eV) of 3.2–3.3 eV. The peaks at 3.25 eV are due to the optical photon energy of ZnO. The small peak at 2.35 eV corresponds to the recombination of free electrons with holes via interstitial zinc, or via defects at the grain boundary [22, 23]. A strong PL peak, centered at 3.2–3.3 eV, corresponds to the near photon energy edge emission at 3.25 eV.

Figure 5(a–e) show surface morphology, as analyzed by AFM microscopy, of ZnO films deposited at different H_2/Ar mole ratios. In the case of the sample deposited at $H_2/Ar = 0$, the corresponding image (Fig. 1a) shows a porous surface morphology composed of grained separated by voids. For films deposited at H_2/Ar ranging from 0.15 to 0.6, AFM images in Fig. 4(b–e) reveal the growth of grains, both isolated and those agglomerated to form bigger grains. By increasing the H_2/Ar mole ratio, the root mean square (RMS) roughness first decreases, and then increases, reaching a minimum value of 5.3 at $H_2/Ar = 0.3$. This indicates that the smoothest surface is obtained at that ratio. The highest RMS roughness, observed at $H_2/Ar = 0$, is caused by the unstable decomposition of DEZn. Increasing the H_2/Ar ratio increases the decomposition of DEZn as well as the mobility of deposited ions resulting in a lower RMS roughness. For H_2/Ar mole ratios over 0.3, the etching effect dominates the surface morphology.

Figures 6 and 7 show the chemical analysis of the films carried out by the complementary XPS and RBS techniques. In the case of XPS, the analyses were conducted after cleaning of the samples by a mild sputtering treatment to remove any organic contamination due to adsorption from the atmosphere. After this surface cleaning, only Zn and O atoms were present on the surface of the films, indicating that the organometallic precursors were fully decomposed and the by-products (CO_2, CH*x*, EtOH, etc.) were released to the gas phase during deposition. The chemical state of the ZnO film surface prepared by ECR-

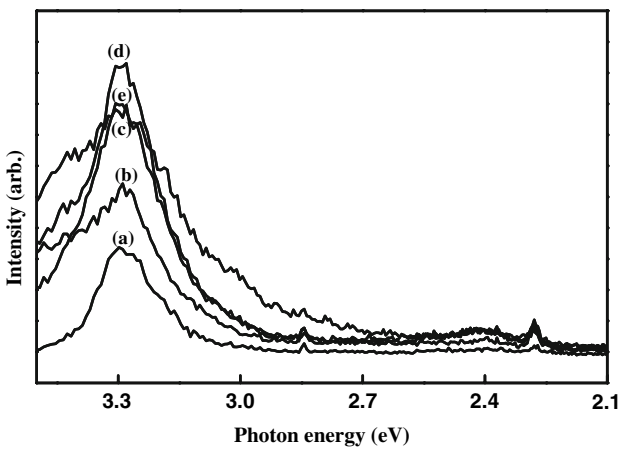

Fig. 4 Photoluminescence spectra of ZnO films at various H_2/Ar ratios: (**a**) 0, (**b**) 0.15, (**c**) 0.3, (**d**) 0.45 and (**e**) 0.6

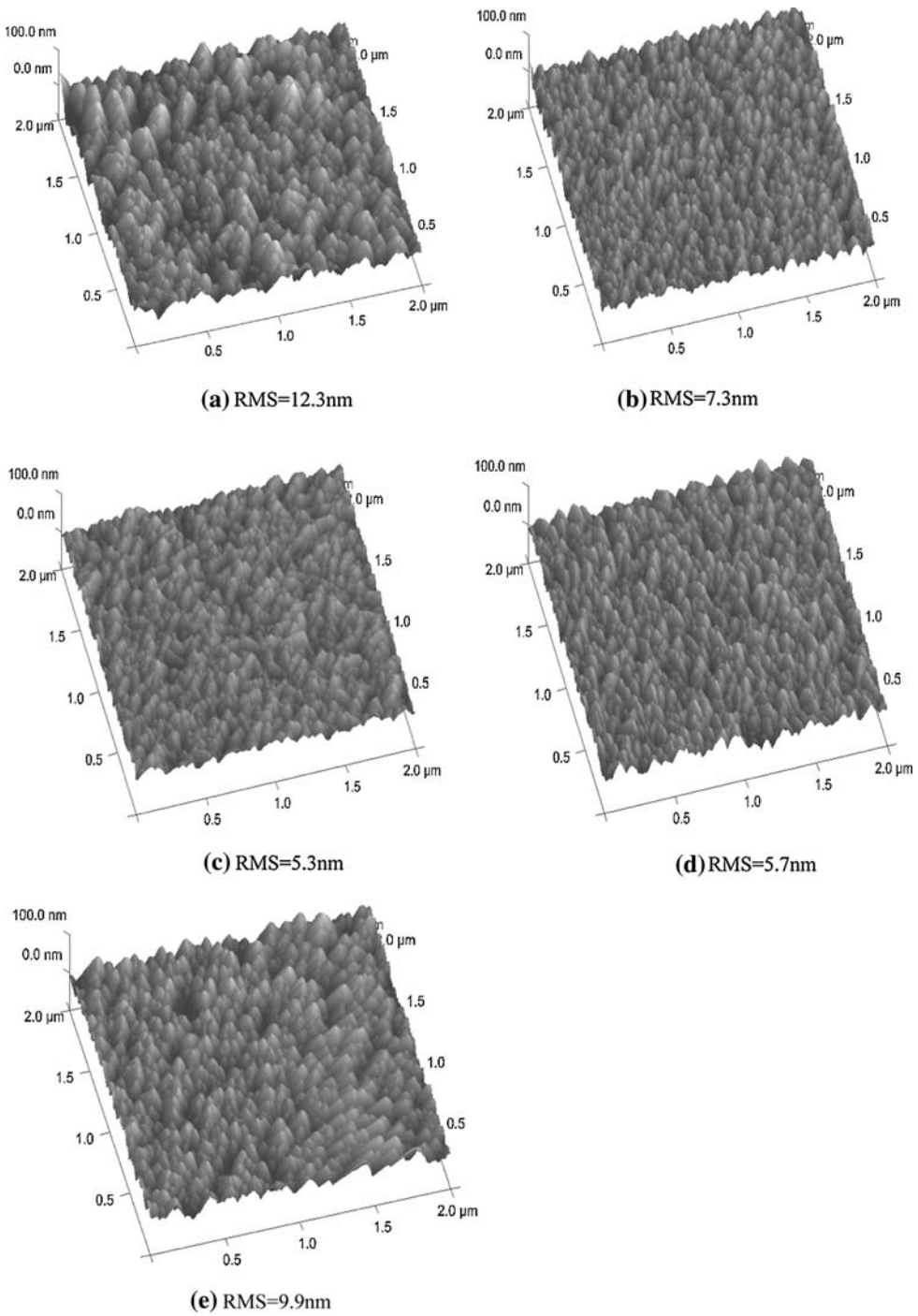

Fig. 5 Three-dimensional topography obtained by atomic force microscopy of ZnO films prepared at different H_2/Ar ratio: (**a**) 0, (**b**) 0.15, (**c**) 0.3, (**d**) 0.45 and (**e**) 0.6

CVD was analyzed by XPS. The spectra of C1s, O1s, Zn2p3 obtained are shown in Fig. 6. The C1s spectrum for the ZnO deposited film by ECR-CVD consisted of three distinct peaks: C–H (285 eV), C–O (286.4–287.0 eV), C=O (288–288.4 eV). Oxidized zinc (530 eV) and the O=C bond (532 eV) appear in the O1s spectrum. As a result of curve fitting for the Zn2p3 spectrum, the Zn2p1 (1043.89 eV) and Zn2p3 (1022.1 eV) peaks were isolated. It was also found that the electronic parameters for the Zn (Zn2p3: 1021 eV, $Zn_{L3M45M45}$: 988 eV) and O (O1s: 530 eV) signals are similar to those found for ZnO.

As shown in Fig. 7, RBS analysis of a selected group of films deposited on PET showed that elemental Zn and O were observed inside the films, in agreement with results obtained by XPS in Fig. 6. RBS also showed that the ZnO molecules were homogeneously distributed in the depth direction and that there is a clear correlation between zinc and oxide content.

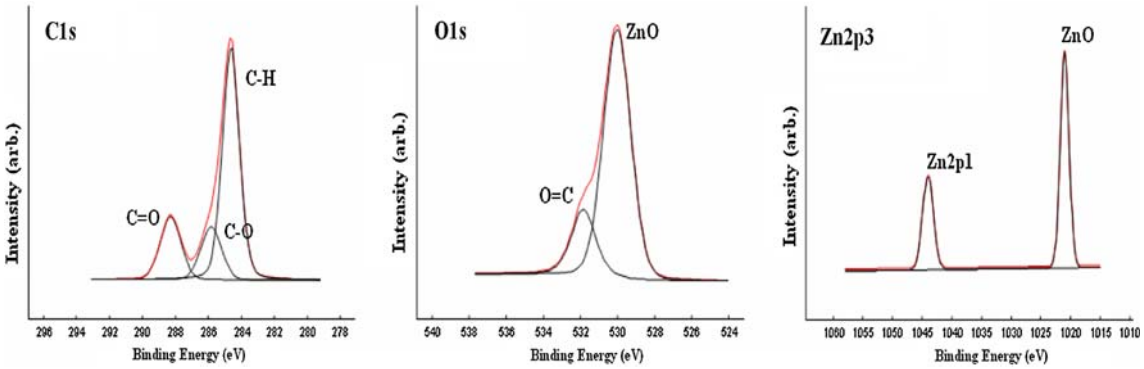

Fig. 6 Peaks of chemical binding energy from the XPS of ZnO films deposited on the PET substrate

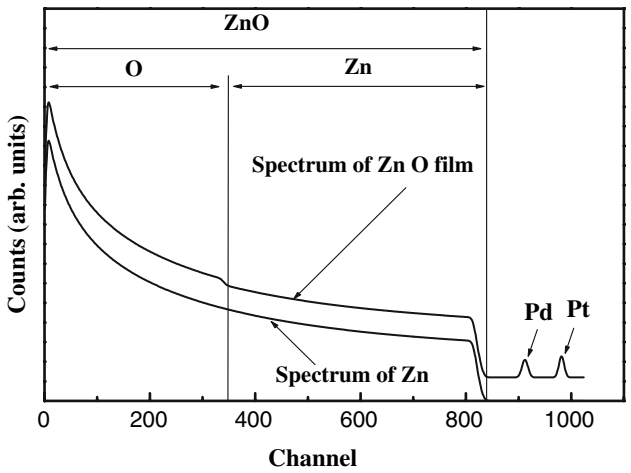

Fig. 7 Composition, thickness and distribution of ZnO inside the films obtained by Rutherford back scattering for a small set of sample

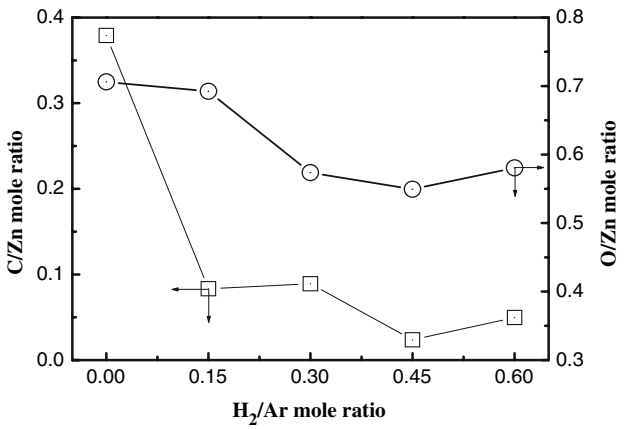

Fig. 8 The composition of the films determined by XPS as a function of H_2/Ar mole ratio

The atomic ratios of both oxide and carbon to metal zinc in the films prepared as a function of an H_2/Ar mole ratio, determined from RBS and XPS measurement of Fig. 6 and Fig. 7, and normalized as ZnO are shown in Fig. 8. Without the addition of hydrogen, the plasma polymerization of the diethyl functional group leads to the formation of carbon rich surface layer in the ZnO film. The C/Zn mole ratio of the films decreases gradually with the increase in hydrogen content. The reason for these results can be explained by the increase in partial pressure of hydrogen in the plasma that generates of the more hydrogen ions through the inelastic collisions in the plasma. These hydrogen ions lead to the formation of stable volatile organic compounds such as CH_4, C_2H_4, C_2H_6, alcohol, CO, CO_2, OH, etc., by a gas phase substitution reaction with DEZn. The O/Zn ratio was non-symmetrical stoichiometric and in the range of 0.5–0.7. The highest O/Zn ratio was observed at zero hydrogen content, and it decreased slightly with an increase of the H_2/Ar mole ratio. In consequence, the addition of hydrogen to the plasma leads to Zn-rich ZnO films.

The ZnO films with a stoichiometric mole ratio of zinc and oxygen have the insulator properties, but on the other hand it becomes as a conductor according to non-symmetrical stoichiometry of zinc and oxide. Therefore the electrical properties of ZnO are strongly influenced by process conditions that may change of the deposited composition. Figure 9 shows the Hall mobility and electrical resistivity of the ZnO films on the PET films, which were measured respectively by a Hall measurement system and the 4-point probe method at room temperature. As the H_2/Ar ratio increases from 0 to 0.6, the film resistivity decreases and reaches a minimum value of 2.5×10^{-2} Ω cm. Increase of the H_2/Ar ratio leads to highly conducting ZnO films. The Hall mobility increases gradually from 8.0 to 34.0 $cm^2\ V^{-1}\ s^{-1}$ as the H_2/Ar ratio increases from 0 to 0.6. However, with an increase of thickness of the ZnO layer from 400 to 600 nm, surface resistivity of the film decreased. The increase in film thickness caused by the hydrogen content resulted from the enhanced decomposition of DEZn under an ECR plasma atmosphere. Table 2 also shows that hole and electron concentration increase with the H_2/Ar. Thus hydrogen content plays an

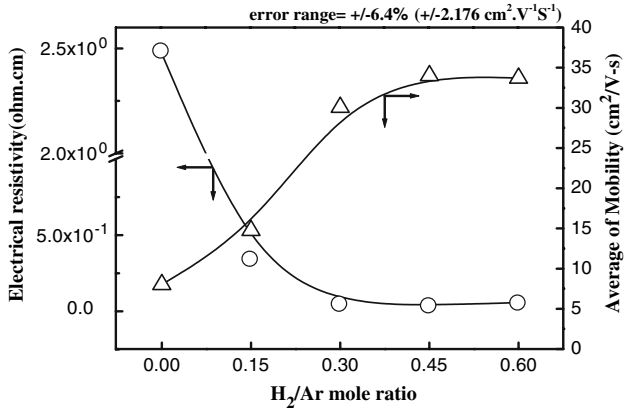

Fig. 9 Effect of the H_2/Ar mole ratio on electrical resistivity and average of mobility of ZnO film

Table 2 Hole and electron concentrations for ZnO film deposited at different H_2/Ar ratios

H_2/Ar mole ratio	Hole concentration (cm^{-3})	Electron concentration (cm^{-3})
0	4.78×10^{19}	1.43×10^{15}
0.15	6.42×10^{19}	2.04×10^{15}
0.3	1.52×10^{20}	3.21×10^{15}
0.45	1.82×10^{20}	5.74×10^{15}
0.6	1.67×10^{20}	5.82×10^{15}

important role in increasing the Hall mobility, hole concentration and electron concentration.

Conclusions

Effect of the hydrogen content on the characteristics of zinc oxide film prepared on PET substrate at room temperature using the ECR - CVD system was investigated. The ZnO film has a polycrystalline hexagonal wurtzite structure that corresponds to the (100), (002), (101), and (110) faces. Zinc oxide films of good electrical and optical property require H_2/Ar ratios of about 0.45. A rough surface with large grains was obtained for films deposited at H_2/Ar ratios of 0.45 and 0.6. The atomic concentrations of Zn and O were uniform across the film thickness, but the composition ratio of Zn and O varied with the H_2/Ar concentration in the range of 0.5–0.7. Hall mobility increased with a lower of O/Zn ratio, which related closely to the hydrogen content. The highest Hall mobility of 34.0 $cm^2\ V^{-1}\ S^{-1}$ and carrier concentration of $5.74 \times 10^{15}\ cm^{-3}$ were observed at an O/Zn ratio of 0.56. The zinc oxide atoms were homogeneously distributed in the depth direction and a distinctive interface between the ZnO film and PET substrate was observed. The observed maximum transmittance and electrical resistivity were over 90% and $2.5 \times 10^{-2}\ \Omega$ cm, respectively, in the experimental range studied.

Acknowledgement The authors would like to thank Professor P.L. Silveston of Univ. of Waterloo for his review of the manuscript.

References

1. Brown HE (1957) Zinc oxide rediscovered. The New Jersey Zinc Company, New York, pp 10–34
2. Zafar SA (1997) Growth and characterization of thin film ZnO and (In,Ga)Se_2 for photovoltaic applications. MS Thesis, University of South Florida, Tampa, FL, USA
3. Vossen JL, Kern W (1978) Thin film processes. Academic Press, p 25
4. http://www.i-w-t.com/john_hall_first.html, Accessed 16 Dec 2006
5. Oleti Kalki Rajan M (2004) Characterization of P-type films. Master degree Dissertation, Dept. of Electrical Eng., University of South Florida, USA, pp 1–54
6. Suh KJ, Okada H, Wakahara A, Kim HJ, Chang HJ, Yoshida A(2004) Eng Mat 270–273:878
7. Takata S, Minami T, Nanto H (1981) Jpn J Appl Phys 20:1759
8. Tanaka S, Takahashi K, Sekiguchi T, Sumino K, Tanaka J (1995) J Appl Phys 77:4021
9. Sekiguchi T, Ohashi N, Terada Y (1997) Jpn J Appl Phys, Part 2 36:L289 30
10. Liang WY, Yoffe AD (1968) Phys Rev Lett 20:59
11. Lee J-M, Kim K-K, Park S-J, Park W-K (2001) Appl Phys Lett 78:3842
12. Shul RJ, Lovejoy MC, Baen AG, Zolper JC, Rieger DJ, Hafich MJ et al. (1995) J Vac Sci Technol A 13:912
13. Fujinami Y, Hayashi H, Ebe A, Imai O, Ogata K(1998) Mat Chem Phys 54:102
14. Lim VWL, Kang ET, Neoh KG (2001) Synth Met 123:107
15. Gerenser LJ (1990) J Vac Sci Technol A 8:3682
16. Lee JK, Jeon BJ, Lee S (2006) Mat Sci Forum 510–511:666
17. Jeon BJ, Ko H, Hyun J, Byun D, Lee JK (2006) Thin Solid Films 496:395
18. Jeon BJ, Lee JK (2006) J Mat Sci 41:6274
19. Hsiao C-S, Cheng-H, Chen S-Y, Liou S-C (2006) J Vac Sci Technol B24:288
20. Warren BE (1990) X-ray diffraction. Dover, New York, p 253
21. Stroyuk AL, Shvalagin VV, Kuchmii SY (2005) J Photochem Photobio A: Chem 173:185
22. Park JH, Byun D, Lee JK (2007) Characteristics of zinc oxide thin film on poly ethylene terethalate (PET) substrate prepared by ECR-MOCVD. Intl. Conf. on Display LEDs, pp 19–183, COEX Seoul, Korea, Jan 30–Feb 2
23. Hupkes J, Rech B, Calnan S, Kluth O, Zastrow U, Siekmann H, Wutting M (2004) Proc. 5th Int. Conf. on Coatings on Glass, Saarbrucken, Germany, p 895